THE JOURNAL OF BIOLOGICAL CHEMISTRY VOL. 284, NO. 40, pp. 27370–27376, October 2, 2009
© 2009 by The American Society for Biochemistry and Molecular Biology, Inc. Printed in the U.S.A.

Magnitude of a Conformational Change in the Glycine Receptor β1-β2 Loop Is Correlated with Agonist Efficacy*[S]

Received for publication, July 24, 2009 Published, JBC Papers in Press, July 30, 2009, DOI 10.1074/jbc.M109.048405

Stephan A. Pless[1] **and Joseph W. Lynch**[2]

From the Queensland Brain Institute and School of Biomedical Sciences, University of Queensland, Brisbane QLD 4072, Australia

The efficacy of agonists at Cys-loop ion channel receptors is determined by the rate they isomerize receptors to a pre-open flip state. Once the flip state is reached, the shut-open reaction is similar for low and high efficacy agonists. The present study sought to identify a conformational change associated with the closed-flip transition in the α1-glycine receptor. We employed voltage-clamp fluorometry to compare ligand-binding domain conformational changes induced by the following agonists, listed from highest to lowest affinity and efficacy: glycine > β-alanine > taurine. Voltage-clamp fluorometry involves labeling introduced cysteines with environmentally sensitive fluorophores and inferring structural rearrangements from ligand-induced fluorescence changes. Agonist affinity and efficacy correlated inversely with maximum fluorescence magnitudes at labeled residues in ligand-binding domain loops D and E, suggesting that large conformational changes in this region preclude efficacious gating. However, agonist affinity and efficacy correlated directly with maximum fluorescence magnitudes from a label attached to A52C in loop 2, near the transmembrane domain interface. Because glycine experiences the largest affinity increase between closed and flip states, we propose that the magnitude of this fluorescence signal is directly proportional to the agonist affinity increase. In contrast, labeled residues in loops C, F, and the pre-M1 domain yielded agonist-independent fluorescence responses. Our results support the conclusion that a closed-flip conformation change, with a magnitude proportional to the agonist affinity increase from closed to flip states, occurs in the microenvironment of Ala-52.

Glycine receptors (GlyRs)[3] are pentameric chloride-selective ion channels that mediate fast inhibitory neurotransmission (1). They are members of the Cys-loop receptor family that includes the prototypical nicotinic acetylcholine receptor (nAChR), the γ-aminobutyric acid type-A receptors ($GABA_A$Rs), and serotonin type-3 receptors ($5\text{-}HT_3$Rs). Recent structural studies have provided a wealth of information on the structure and function of this receptor family (2–6). In Cys-loop receptors, the ligand-binding domain (LBD) preceding the four transmembrane helices consists of two twisted β-sheets. The inner (vestibule facing) β-sheet comprises seven β-strands, while the outer β-sheet is formed by three β-strands (3). The ligand binding site is located at the interface of adjacent subunits and is lined by six domains: three loops from the principal and the complementary sides, termed A-C and D-F, respectively (3).

GlyRs are activated by endogenous amino acid agonists in the following order of efficacy: glycine > β-alanine > taurine (7, 8). As these amino acids share considerable structural similarity (Fig. 1*A*), they are likely to compete for the same binding site (9–11). A recent ground-breaking study on an intermediate pre-open state, the so-called "flip" state (12), has provided new insights into the mechanism of partial agonism in Cys-loop receptors (13). This study suggested that agonist efficacy depends on the ability of the agonist to convert the inert agonist-bound receptor to the pre-open flip state. Once the flip state is reached, the shut-open reaction is similar for high and low efficacy agonists. To date there is, however, very little information concerning the structural basis for the lower efficacies of partial agonists. To address this, the present study employed the voltage-clamp fluorometry (VCF) technique (14) to compare the conformational changes induced by glycine, β-alanine, and taurine at various positions in the GlyR LBD.

VCF involves tethering of an environmentally sensitive fluorophore to a cysteine engineered into a domain of interest. If ligand-binding and/or channel opening leads to a changed dielectric environment surrounding the fluorophore, a change in quantum yield or emission spectrum can be detected. VCF was first employed on voltage-gated potassium channels (15) and has since provided a wealth of information on Cys-loop receptor structure and function (16–23). Here we employ VCF to identify an agonist-specific conformational change that may control or reflect the rate at which the GlyR isomerizes to the flip state.

* This work was supported by the Australian Research Council and the National Health and Medical Research Council of Australia (NHMRC).

[S] The on-line version of this article (available at http://www.jbc.org) contains supplemental Fig. S1.

[1] Supported by an International Postgraduate Research Scholarship from the University of Queensland. Present address: Dept. of Anesthesiology, Pharmacology and Therapeutics, University of British Columbia, Vancouver BC V6T 1Z3, Canada.

[2] Supported by an NHMRC Research Fellowship. To whom correspondence should be addressed: Queensland Brain Institute, University of Queensland, Brisbane QLD 4072, Australia. Tel.: 617-3346-6375; Fax: 617-3346-6301; E-mail: j.lynch@uq.edu.au.

[3] The abbreviations used are: GlyR, glycine receptor; $5\text{-}HT_3$R, serotonin type-3 receptor; Δ*F*, change in fluorescence; Δ*I*, change in current; AChBP, acetylcholine-binding protein; AF546, Alexa Fluor 546; EC, extracellular; $GABA_{A/C}$R, GABA type-A/type-C receptor; LBD, ligand-binding domain; MTSR, methanethiosulfonate-rhodamine; MTS-TAMRA, 2-((5(6)-tetramethylrhodamine)carboxylamino)ethyl methanethiosulfonate; nAChR, nicotinic acetylcholine receptor; pre-M1, the domain preceding the first transmembrane segment; TMD, transmembrane domain; TMRM, tetramethylrhodamine-maleimide; VCF, voltage-clamp fluorometry; WT, wild type.

EXPERIMENTAL PROCEDURES

Chemicals—Glycine, taurine, and β-alanine (all Sigma Aldrich) were dissolved in water and stored at 4 °C. Strychnine (Sigma Aldrich), was dissolved in DMSO (Sigma Aldrich) and stored at −20 °C. Sulforhodamine methanethiosulfonate (MTSR) and 2-((5(6)-tetramethylrhodamine)carboxylamino)ethyl methanethiosulfonate (MTS-TAMRA) (Toronto Research Chemicals, North York, ON, Canada) were dissolved in DMSO and stored at −20 °C. Alexa Fluor 546 C_5 maleimide (AF546, Invitrogen Corp.) was dissolved in water on the day of the experiment.

Molecular Biology—The human GlyR α1 cDNA was subcloned into the pGEMHE vector. All constructs contained the functionally silent C41A mutation to remove the only uncross-linked cysteine in the LBD. Site-directed mutagenesis was carried out with the QuikChange mutagenesis kit (Stratagene, La Jolla, CA) and incorporation of mutations was confirmed by automated sequencing. The mMessage mMachine Kit (Ambion, Austin, TX) was used to generate capped mRNA.

Oocyte Preparation, Injection, and Labeling—Oocytes from female *Xenopus laevis* frogs (*Xenopus* Express) were prepared as described (20) and injected with 10 ng of capped mRNA. Oocytes were incubated for 3–5 days at 18 °C in a solution containing 96 mM NaCl, 2 mM KCl, 1 mM $MgCl_2$, 1.8 mM $CaCl_2$, 5 mM HEPES, 0.6 mM theophylline, 2.5 mM pyruvic acid, 50 μg/ml gentamycin (Cambrex Corporation, East Rutherford, NJ), pH 7.4. Prior to recording oocytes were transferred into ND96 (96 mM NaCl, 2 mM KCl, 1 mM $MgCl_2$, 1.8 mM $CaCl_2$, 5 mM HEPES, pH 7.4) containing 5–20 μM dye for 30 s (for MTS-linked dyes) or 45 min (for AF546). Oocytes were washed in ND96 and stored up to 4 h before recording. The GlyR LBD model in Fig. 1 shows the positions of the labeled residues employed in this study. Wild type (WT) GlyRs never displayed detectable ΔF or ΔI changes after incubation with MTS-TAMRA (Table 1) or any of the other fluorophores employed here ($n = 3$ each, data not shown). We thus rule out nonspecific effects of the fluorophores.

VCF and Data Analysis—The VCF set up has previously been described in detail (20). In brief, an inverted microscope (Nikon Instruments, Kawasaki, Japan) was fitted with a high-Q tetramethylrhodamine isothiocyanate filter set (Chroma Technology, Rockingham, VT), a Plan Fluor 40× objective (Nikon Instruments, Kawasaki, Japan), a PhotoMax 200 photodiode (Dagan Corporation, Minneapolis, MN), a xenon arc lamp (Sutter Instruments, Novato, CA) and an automated perfusion system (AutoMate Scientific, San Francisco, CA). A detailed description of the recording chamber can be found in Ref. 17. Electrodes for two-electrode voltage clamp recordings were operated by automated micromanipulators (Sutter Instruments, Novarto, CA). All cells were voltage-clamped at −40 mV and current recordings were made with a Gene Clamp 500B amplifier (Axon Instruments, Union City, CA). Fluorescence and current traces were acquired at 200 Hz with a Digidata 1322A interface and digitally filtered at 2 Hz with an eight-pole Bessel filter for analysis and display (Axon Instruments, Union City, CA). Fluorescence baselines were corrected for bleaching where necessary. Values for half-maximal concentrations (EC_{50}) and Hill coefficients (n_H) for ligand-induced activation of current and fluorescence signals were obtained with the Hill equation, fitted with a non-linear least squares algorithm (SigmaPlot 9.0, Systat Software, Point Richmond, CA). All results expressed as means ± S.E. of at least three independent experiments. The molecular model was generated with PyMOL 0.99 (DeLano Scientific LLC, San Francisco, CA).

RESULTS

GlyRs exhibit the agonist efficacy (and affinity) sequence: glycine > β-alanine > taurine (7, 8). When α1-GlyRs are expressed in mammalian HEK293 cells, the efficacies of all three agonists are relatively high so that taurine and β-alanine act as full or near-full agonists (7, 9, 24). However, when expressed in *Xenopus* oocytes, the efficacies of all three agonists are reduced, which results in an increase in their EC_{50} values and a conversion of β-alanine and taurine into weak partial agonists relative to glycine (8). Because the reduced efficacies seen in oocyte-expressed GlyRs can be reversed by expressing receptors at high densities (9, 25), we injected oocytes with a high amount (10 ng) of mRNA to ensure that β-alanine and taurine evoked maximal currents that were comparable in magnitude to those elicited by glycine. To facilitate comparison of agonist-induced responses, the maximum currents (ΔI_{max}) and maximum fluorescence changes (ΔF_{max}) elicited by β-alanine and taurine at all labeled residues investigated here were normalized to those elicited by glycine via the relations, $R_I = (\Delta I_{max(\beta\text{-Ala or tau})})/(\Delta I_{max(Gly)})$ and $R_F = (\Delta F_{max(\beta\text{-Ala or tau})})/(\Delta F_{max(Gly)})$, respectively. In this nomenclature, *R* refers to ratio and subscripts *I* and *F* refer to current and fluorescence, respectively. These values are summarized in Table 1 for the WT and each mutant GlyR investigated here.

Conformational Changes in the Inner β-Sheet—We investigated labeled residues in three domains of the LBD inner β-sheet: loop D, loop E, and loop 2 (Fig. 1*B*). Loop D contributes to the complementary (−) side of the GlyR-binding pocket (11, 26). As shown in Fig. 1*B*, Loop D forms part of β-strand 2 that in turn forms part of the inner β-sheet. We recently demonstrated that the MTS-TAMRA-labeled Q67C residue in loop D reports a much smaller ΔF_{max} in response to saturating glycine (Fig. 2*A*) than to strychnine (27). Here we quantitated the ΔF and ΔI dose-response relationships for both β-alanine and taurine (Table 1 and Fig. 2, *B* and *C*, supplemental Fig. S1). Importantly, the mean ΔI_{max} values for glycine, β-alanine, and taurine at this mutant GlyR were indistinguishable in magnitude (Fig. 2*D*). While the ΔI EC_{50} values for all three agonists were increased in the labeled Q67C GlyR relative to their WT GlyR values, their rank order was unchanged implying that the mutation did not affect the agonist affinity or efficacy sequence (Table 1). However, taurine activated the largest ΔF_{max} signals, which were only marginally smaller than those induced by the antagonist, strychnine ($R_{F(strychnine)} = 11.8 \pm 2.1$ *versus* $R_{F(taurine)} = 11.1 \pm 0.2$, both $n = 4$). The agonist-activated ΔF_{max} values decreased significantly from taurine to β-alanine and from β-alanine to glycine (Fig. 2*D*). The strong linear correlation between ΔI EC_{50} and ΔF_{max} values for the three tested agonists ($R^2 = 0.89$), demonstrates that the ΔF_{max} reported by the labeled Q67C is inversely related to both agonist efficacy and affinity.

TABLE 1

Summary of results for glycine, β-alanine, and taurine-evoked current and fluorescence recordings

Displayed are values for half-maximal activation (EC_{50}), Hill coefficient (n_H), maximal current, and fluorescence responses for glycine (DI_{max} and DF_{max}) and those for β-alanine and taurine, normalized to glycine responses ($R_{I/F} = (I/F_{max(b\text{-}ala\ or\ tau)})/(I/F_{max(gly)})$). †/‡ indicate significant differences to glycine (†) and β-alanine (‡) evoked current EC_{50} values ($p < 0.05$, Student's *t*-test). */# indicate significant differences to maximal glycine (*) and β-alanine (#) evoked current and fluorescence responses ($p < 0.05$, Student's *t*-test). $n = 3–9$ for each experiment. Numbers in superscript indicate the fluorophore used: [1], MTS-TAMRA; [2], MTSR; [3], AF546. All results for fluorescence are shown in bold. Note that all values for glycine-evoked current and fluorescence responses are reproduced from Pless and Lynch (27).

Construct	Glycine			β-Alanine			Taurine		
	EC_{50}	n_H	$I_{max}/\Delta F_{max}$	EC_{50}	n_H	R_I/R_F	EC_{50}	n_H	R_I/R_F
	μM		μA/%	μM			μM		
WT									
WT Δ*I* no label	15.5 ± 0.3	2.6 ± 0.1	8.3 ± 0.4	22.2 ± 0.1†	2.4 ± 0.1	0.97 ± 0.03	64.4 ± 1.0†/‡	2.2 ± 0.1	0.94 ± 0.02
WT Δ*I* label[1]	15.6 ± 0.4	2.7 ± 0.1	7.9 ± 0.2	20.8 ± 0.2†	2.5 ± 0.1	0.97 ± 0.02	60.4 ± 1.5†/‡	2.5 ± 0.1	0.98 ± 0.02
Loop E									
L127C Δ*I*[1]	4950 ± 180	2.4 ± 0.2	7.7 ± 0.8	6690 ± 140†	2.7 ± 0.1	1.04 ± 0.10	18400 ± 100†/‡	2.8 ± 0.1	1.00 ± 0.12
L127C Δ*F*	**6070 ± 240**	**1.8 ± 0.1**	**46.7 ± 7.1**	**47100 ± 3300**	**1.2 ± 0.1**	**2.67 ± 0.35***	**66100 ± 4600**	**1.2 ± 0.1**	**3.19 ± 0.41***
Loop D									
Q67C Δ*I*[1]	63.1 ± 0.6	2.9 ± 0.1	7.2 ± 0.5	240 ± 6†	2.4 ± 0.1	1.11 ± 0.19	665 ± 10†/‡	2.3 ± 0.1	0.92 ± 0.04
Q67C Δ*F*	**1180 ± 50**	**1.7 ± 0.1**	**18.0 ± 0.6**	**2440 ± 150**	**1.2 ± 0.1**	**7.20 ± 0.78***	**3000 ± 90**	**1.2 ± 0.1**	**11.38 ± 1.50*/#**
Loop 2									
A52C Δ*I*[1]	17.4 ± 0.1	3.0 ± 0.1	7.7 ± 0.2	40.8 ± 0.3†	2.6 ± 0.1	0.85 ± 0.13	105 ± 1†/‡	2.1 ± 0.1	0.99 ± 0.15
A52C Δ*F*	**201 ± 10**	**1.4 ± 0.1**	**−8.6 ± 1.1**	**380 ± 38**	**0.9 ± 0.1**	**0.42 ± 0.02***	**730 ± 76**	**1.1 ± 0.1**	**0.23 ± 0.01*/#**
Loop F									
V178C Δ*I*[3]	40.7 ± 0.1	2.6 ± 0.1	10.3 ± 2.3	97.8 ± 9.6†	1.8 ± 0.3	0.85 ± 0.22	400 ± 18†/‡	1.7 ± 0.1	1.11 ± 0.22
V178C Δ*F*	**313 ± 20**	**1.3 ± 0.1**	**12.6 ± 0.6**	**131 ± 1**	**1.4 ± 0.1**	**0.95 ± 0.15**	**283 ± 19**	**1.3 ± 0.1**	**0.84 ± 0.13**
G181C Δ*I*[2]	39.8 ± 1.3	1.9 ± 0.1	9.9 ± 2.1	121 ± 4†	2.3 ± 0.2	0.95 ± 0.10	351 ± 16†/‡	1.7 ± 0.1	0.92 ± 0.08
G181C Δ*F*	**503 ± 65**	**1.3 ± 0.2**	**11.6 ± 2.7**	**553 ± 20**	**1.4 ± 0.1**	**0.92 ± 0.24**	**1400 ± 170**	**1.2 ± 0.1**	**0.88 ± 0.19**
Loop C									
H201C Δ*I*[1]	16.3 ± 0.6	2.9 ± 0.2	9.3 ± 0.8	62.3 ± 0.1†	4.6 ± 0.1	1.26 ± 0.07	117 ± 3†/‡	2.6 ± 0.2	0.82 ± 0.07
H201C Δ*F*	**126 ± 3**	**2.1 ± 0.1**	**10.2 ± 1.0**	**209 ± 39**	**1.3 ± 0.1**	**0.95 ± 0.12**	**365 ± 34**	**1.2 ± 0.1**	**0.78 ± 0.12**
N203C Δ*I*[1]	45.7 ± 1.2	3.0 ± 0.2	6.9 ± 0.2	56.1 ± 1.9†	3.3 ± 0.2	0.93 ± 0.04	90.8 ± 4.2†/‡	2.6 ± 0.4	0.89 ± 0.06
N203C Δ*F*	**526 ± 25**	**1.2 ± 0.1**	**44.3 ± 5.9**	**228 ± 14**	**0.8 ± 0.1**	**0.92 ± 0.07**	**286 ± 15**	**0.8 ± 0.1**	**0.90 ± 0.14**
Pre-M1									
Q219C Δ*I*[2]	9.2 ± 0.2	2.6 ± 0.2	8.4 ± 0.4	12.3 ± 1.3	2.1 ± 0.4	0.86 ± 0.09	22.3 ± 0.4†/‡	2.6 ± 0.1	0.84 ± 0.07
Q219C Δ*F*	**98.6 ± 9.9**	**1.5 ± 0.2**	**−13.3 ± 0.8**	**69.3 ± 5.2**	**1.1 ± 0.1**	**0.90 ± 0.13**	**90.8 ± 5.0**	**1.3 ± 0.1**	**0.81 ± 0.13**
M227C Δ*I*[3]	13.1 ± 0.1	2.4 ± 0.1	6.5 ± 0.5	28.8 ± 0.7†	2.1 ± 0.1	0.79 ± 0.02	81.5 ± 1.9†/‡	2.0 ± 0.1	0.75 ± 0.12
M227C Δ*F*	**226 ± 24**	**1.0 ± 0.1**	**−3.5 ± 0.3**	**98.5 ± 4.6**	**1.1 ± 0.1**	**1.10 ± 0.06**	**336 ± 36**	**1.1 ± 0.1**	**1.13 ± 0.09**

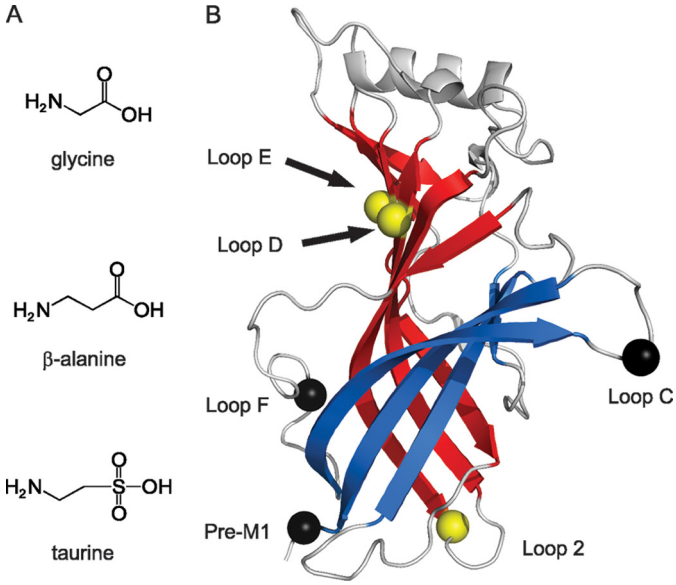

FIGURE 1. *A*, structures of glycine, β-alanine, and taurine. *B*, model of the LBD, based on carbomylcholine-bound AChBP (PDB code 1uv6). The inner β-sheet is displayed in *red*, the outer β-sheet in *blue*. Connecting loops are shown in *gray*. *Colored balls* represent approximate locations of selected residues labeled in regions flanking the outer β-sheet (*black*, G181C in loop F; N203C in loop C; Q219C in the pre-M1 domain) and in the inner β-sheet (*yellow*, L127C in loop E; Q67C in loop D; A52C in loop 2).

Although the Δ*I* EC_{50} values for activation by glycine, β-alanine, and taurine were significantly lower than the corresponding Δ*F* EC_{50} values (Table 1 and supplemental Fig. S1), both current and fluorescence responses were apparent at low glycine concentrations (Fig. 2, *A–C*). Furthermore, for each of the three agonists, the n_H values for the Δ*F* dose response were significantly lower than their values for the Δ*I* dose-response (Table 1), indicating substantially lower cooperativity for Δ*F* signals than for Δ*I* signals. Indeed, this phenomenon applied to all mutants investigated in this study. The reasons for this will be considered in the "Discussion."

We next investigated MTS-TAMRA-labeled L127C in loop E. This domain forms part of β-strand 6 on the inner β-sheet (3, 11). We recently demonstrated that while glycine and strychnine both evoke large ΔF_{max} responses at this labeled site, those activated by strychnine were around four times larger than those activated by glycine (27). This prompted us to conclude that the two ligands induce distinct local conformational rearrangements at this site. In the present study, we found that β-alanine and taurine both induce large Δ*I* and Δ*F* responses (Table 1). The ΔI_{max} values were virtually identical for glycine, β-alanine, and taurine, while the ΔF_{max} signals for β-alanine and taurine were significantly (~3 times) larger than those elicited by glycine (Table 1). The pattern of Δ*I* and Δ*F* responses observed at the labeled L127C residue was therefore similar to that observed at Q67C in the adjacent β-strand, where ΔF_{max} responses were also inversely related to agonist efficacy.

We also found that for both β-alanine and taurine the Δ*I* EC_{50} was significantly lower than that for Δ*F* (Table 1 and supplemental Fig. S1). Additionally, for all three agonists the n_H for Δ*F* was significantly lower that that for Δ*I* (Table 1). It should be

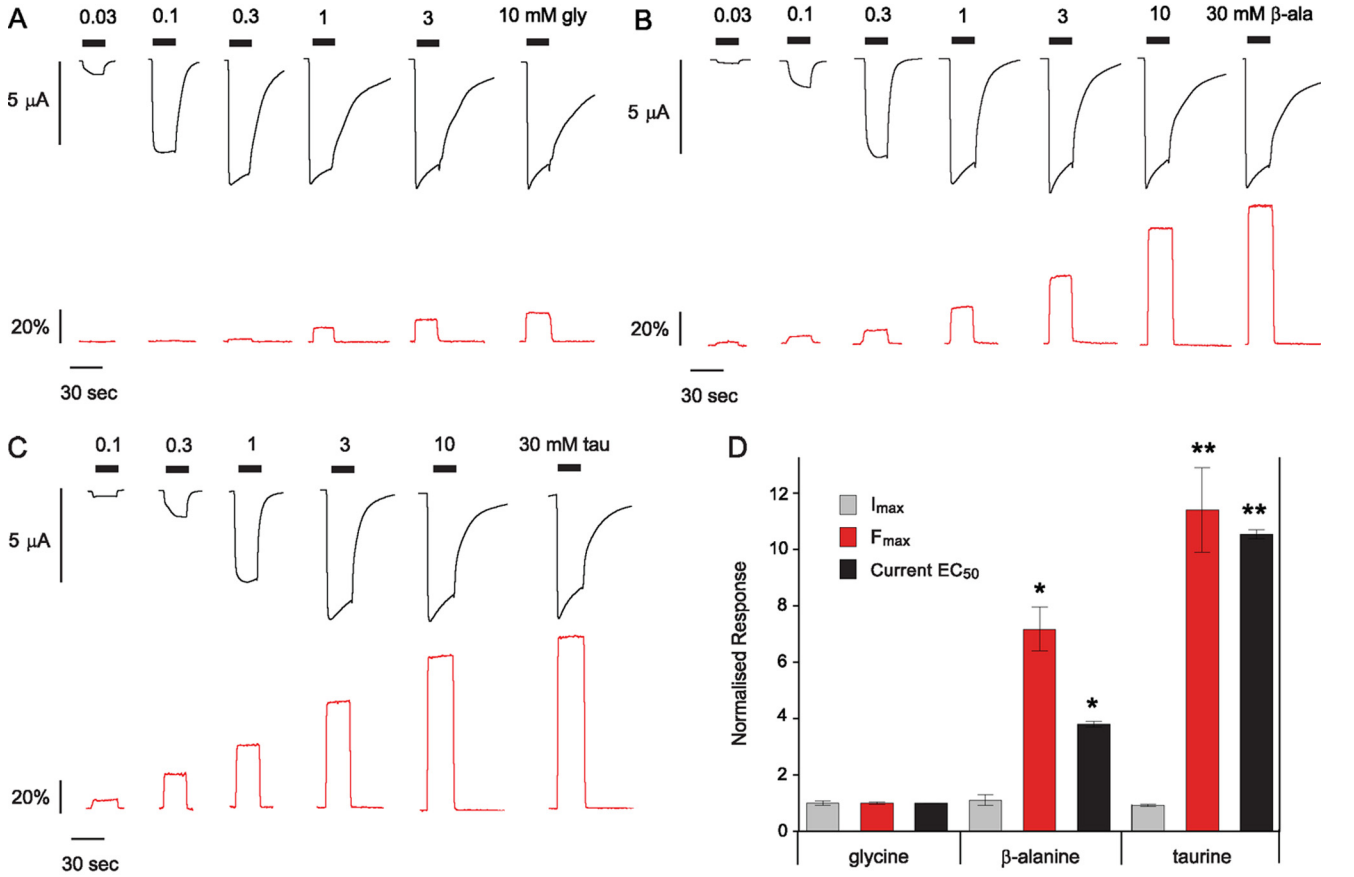

FIGURE 2. **Different agonists induce distinct conformations in loop D in the inner β-sheet.** *A–C*, current (*black*) and fluorescence (*red*) traces recorded from oocytes injected with Q67C during application of glycine (*A*), β-alanine (*B*), and taurine (*C*) (traces in *A* modified from Ref. 27). *D*, comparison of agonist-induced maximal current (I_{max}, *gray*), maximal fluorescence (ΔF_{max}, *red*), and current EC_{50} (*black*). Data normalized to mean values obtained for glycine (27). *Asterisks* indicates significant difference to glycine values (*, $p < 0.005$, Student's *t* test). *Double asterisks* indicates significant difference to both glycine and β-alanine values (**, $p < 0.05$, Student's *t* test).

noted, however, that both ΔI and ΔF responses exhibited similar thresholds at low β-alanine and taurine concentrations.

As loop 2 is also part of the inner β-sheet and is linked to loop D via β-strand 2 (Fig. 1), we investigated the possibility that a label attached to this domain might also report agonist-specific movements. As shown previously (27), the MTS-TAMRA-labeled A52C mutant GlyR yielded reliable ΔF decreases in response to glycine application. A sample ΔI and ΔF dose-response for glycine is shown in Fig. 3*A*, with averaged results presented in Table 1 and supplemental Fig. S1. β-Alanine and taurine application also evoked large ΔI responses but smaller ΔF responses (Fig. 3, *B* and *C* and Table 1). Although all three agonists displayed virtually identical ΔI_{max} values and WT-like ΔI EC_{50} values (Fig. 3*D* and Table 1), the averaged ΔF_{max} values decreased significantly from glycine to β-alanine and from β-alanine to taurine (Fig. 3*D* and Table 1). This trend of ΔF_{max} being directly proportional to agonist efficacy is consistent with our previous finding that the competitive antagonist strychnine induces no measureable ΔF at the labeled A52C GlyR (27). Indeed, there was a strong linear correlation between ΔI EC_{50} and ΔF_{max} values for the three tested agonists ($R^2 = 0.97$), indicating that the local environmental change sensed by the label attached to A52S is directly proportional to agonist affinity and efficacy.

The EC_{50} values of both the glycine- and β-alanine-induced ΔF responses were significantly higher than those of the corresponding ΔI responses (Table 1 and supplemental Fig. S1). In addition, as with the previously described mutants, the n_H values were significantly higher for ΔI compared with ΔF (Table 1).

Loop C, Loop F, and Pre-M1 Domain—Loop C, loop F, and the pre-M1 domain all flank the outer β-sheet of the Cys-loop receptor LBD (Fig. 1*B*). In the present study, we investigated the ligand sensitivity of ΔI and ΔF responses at the following labeled residues: V178C and G181C in loop F, H201C and N203C in loop C, and Q219C and M227C in the pre-M1 domain. The locations of G181C, N203C, and Q219C are shown in Fig. 1*B*. We have previously demonstrated that labels attached to these sites yield robust ΔF values in response to glycine activation (27). The fluorescent labels that were successfully attached to each of these sites are indicated in Table 1. In our previous study, we showed that ΔF_{max} values at most labeled residues in loops F and C were indistinguishable for glycine and strychnine, suggesting these domains mainly undergo local ligand-independent conformational changes (27). In the present study, we found that all six labeled residues also responded with large ΔI and ΔF signals in response to β-alanine and taurine application (supplemental Fig. S1 and Table

1). Indeed, glycine, β-alanine, and taurine induced virtually identical ΔI_{max} and ΔF_{max} values at all six labeled residues (Table 1 and Fig. 4), indicating that agonist-induced movements in loop F, loop C, and in the pre-M1 domain do not discriminate between different agonists. This is an important finding, as we previously showed that H201C in loop C and Q219C and M227C in the pre-M1 domain did discriminate between glycine and strychnine (27).

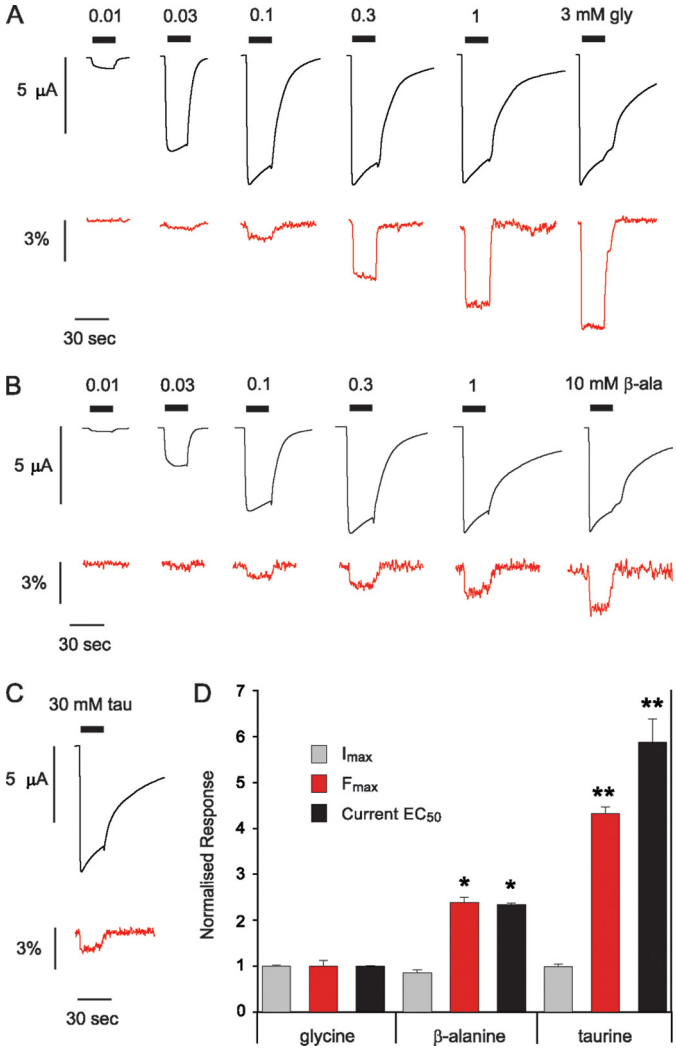

FIGURE 3. **Different agonists induce distinct conformations in loop 2 in the inner β-sheet.** *A–C*, current (*black*) and fluorescence (*red*) traces recorded from oocytes injected with A52C during application of glycine (*A*), β-alanine (*B*), and taurine (*C*) (traces in *A* modified from Ref. 27). *D*, comparison of agonist-induced maximal current (ΔI_{max}, *gray*), maximal fluorescence (ΔF_{max}, *red*), and current EC_{50} (*black*). Note that the F_{max} values have been inverted to facilitate comparison. Data normalized to mean values obtained for glycine (27). *Single asterisks* indicate significant difference to glycine values (*, $p <$ 0.0005, Student's *t* test). *Double asterisks* indicates significant difference to both glycine and β-alanine values (**, $p < 0.0005$, Student's *t* test).

DISCUSSION

Ligand-specific Movements in the Inner β-Sheet—ΔF values can be produced by either fluorophore environmental changes or by direct quench/dequench interactions between ligand and fluorophore. A direct ligand-fluorophore interaction cannot explain results from labeled residues in loop 2 or the pre-M1 domain as they lie well away from the ligand-binding site. Direct interactions between fluorophore and ligand are difficult to categorically rule out for the remaining labeled residues in binding loops C, D, E, and F. However, many of the sites investigated here have been studied previously in VCF studies on Cys-loop receptors and in each case a variety of criteria has been used to rule out direct ligand-induced quenching or dequenching events (16, 19, 21, 22, 27).

For almost all labeled residues examined here, the ΔF dose-response relationship was right-shifted with a shallower slope relative to the corresponding ΔI dose-response relationship. We propose that this is because the binding of three glycine molecules is sufficient for a maximal ΔI (7, 28, 29), whereas ΔF, which responds to local conformational changes or individual binding events, does not reach a maximum until five glycine molecules are bound. Importantly, we assume that significantly different ΔF_{max} values for labeled loop 2 or pre-M1 residues indicate distinct local conformational rearrangements.

All three agonists plus strychnine induced large ΔF increases at the labeled Q67C and L127C residues. These residues are located adjacent to each other in loops D and E of the inner β-sheet. Because glycine, β-alanine, and taurine elicit identical single channel conductances (7) and activated identical ΔI_{max} values at all labeled mutant receptors examined here (Table 1), we conclude that the mean number of receptors activated by the different agonists remains constant. Thus, the dramatically different ΔF_{max} values for each of the three agonists at the labeled Q67C and L127C GlyRs provide strong evidence for an agonist-specific fluorophore interaction or agonist-specific conformational rearrangements in loops D and E. The increase in ΔF that occurs upon ligand binding is consistent with an increased hydrophobicity of the fluorophore environment. Hence, results from loops D and E are consistent with the long-held view of a ligand-induced closure of the binding pocket (16, 19, 30–32), which should increase hydrophobicity within the binding site. Our experiments demonstrate an inverse relationship between agonist efficacy (or affinity) and ΔF_{max} at both labeled sites in loops D and E. They also show that strychnine, which has no agonist efficacy, produces the largest ΔF_{max} at both sites. Together, these results suggest that domain movements associated

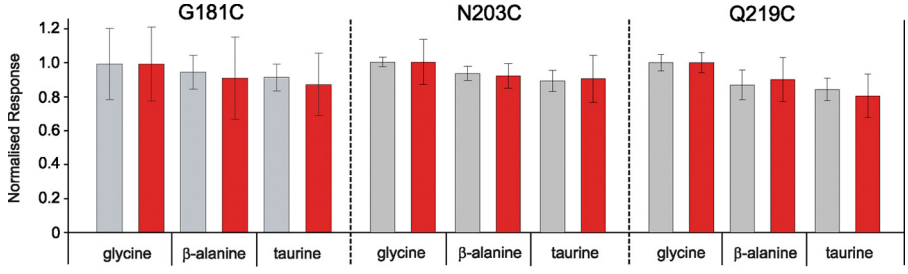

FIGURE 4. **Different agonists induce identical conformations in loops flanking the outer β-sheet (loop F and loop C) and in the pre-M1 domain.** Shown is a comparison of agonist-induced ΔI_{max} (*gray*) and ΔF_{max} (*red*) responses from G181C (loop F), N203C (loop C), and Q219C (pre-M1 domain). Data normalized to mean values obtained for glycine (27).

with large ΔF_{max} increases in loops D and E are not optimal for efficacious channel gating.

Although the A52S startle disease mutation in loop 2 of the inner β-sheet produced an increase in the glycine EC_{50} (33), we found that the A52C mutation had no such effect, even after labeling with MTS-TAMRA (27). Because of its distance from the ligand-binding site, we conclude that the agonist-induced ΔF values elicited from the label attached to this site report a conformational change that either leads to, or occurs as a result of, receptor activation. The lack of a strychnine-induced ΔF at this position supports this interpretation. Agonists invariably produced a decrease in fluorescence suggesting that the label experiences a more hydrophilic environment in the agonist-bound state. This is consistent with the results of a recent study that showed that agonists produce an increase in surface accessibility of the introduced sulfhydryl group in the D43C mutant α7 nAChR, where Asp-43 aligns with the GlyR Ala-52 residue (34). The finding that glycine, β-alanine, and taurine all evoke identical maximal currents but dramatically different ΔF_{max} values lead us to conclude that these agonists induce distinct conformational changes in either loop 2 or its immediate surroundings.

Interpretation of Loop 2 Conformational Changes—A groundbreaking study by Gouaux and co-workers (35) demonstrated that another ligand-gated ion channel, the GluR2 glutamate receptor, displays agonist-specific conformational changes in the ligand-binding domain. In this receptor, the degree of domain closure around the binding site correlated strongly with agonist efficacy. This raises the question as to whether agonist efficacy at Cys-loop receptors may also be graded according to the magnitude of displacement of a domain involved in receptor binding or gating. Although structural studies have provided evidence for ligand-specific conformations around the AChBP-binding pocket (31, 36) and a VCF study provided evidence for ligand-specific conformational changes in the GlyR transmembrane domain (20), our results from loop 2 provide the first evidence from any Cys-loop receptor for a correlation between agonist efficacy and domain movement.

Partial agonism in Cys-loop receptors is due to a propensity for low efficacy agonists to be ineffective at converting the agonist-bound closed receptor to an intermediate pre-open state, dubbed the "flip" state (13). Once the flip state is reached, a high efficacy agonist (glycine) and a low efficacy agonist (taurine) induced very similar rates of transition between flip (shut) and open states (13). Single channel kinetic analysis of the A52S mutant GlyR suggested that this mutation selectively reduced the affinity of glycine for the flip state (33). Thus, glycine-bound A52S mutant GlyRs are less likely to enter the flip state, although once they do, the receptors gate normally. The authors of the flip hypothesis suggested that flipping might correspond to the degree of domain movement around the bound ligand (13, 33).

The α1-GlyR agonist affinity and efficacy sequences both follow the rank order: glycine > β-alanine > taurine (7). Glycine, β-alanine, and taurine also exhibit a progressive increase in length from their amino to hydroxyl ends (Fig. 1*A*). As agonist size is related inversely to both affinity and efficacy, if a ΔF_{max} signal is also correlated with agonist size, it is difficult to ascertain whether the underlying conformational change is associated with an agonist binding interaction or a channel gating conformational change, or both. However, two considerations are worthy of note. First, if the label attached to A52C were detecting a conformational change associated exclusively with the open state (or the flipped state), then glycine and taurine should elicit similar ΔF_{max} values because both agonists produce similar transition rates between the flip and open states (13). Because taurine and glycine produced very different ΔF_{max} signals at A52C, it is more likely that the attached label is detecting a local agonist-induced conformational change that enables flipping to take place. Because glycine promotes flip much more efficiently than taurine (with β-alanine intermediate between the two), this conformational change must be agonist-dependent.

The second consideration is that a single channel kinetic analysis concluded that the conservative A52S mutation selectively reduced the glycine affinity increase in the flip state, thereby reducing the rate of isomerization to that state (33). The authors concluded that the mutation imposed a local structural change that had a long distance effect at the binding site. This finding, which directly implicates Ala-52 in an agonist efficacy-dependent conformation change, is a particularly relevant result as our study is drawing conclusions from a label attached to the same mutated residue.

Taking these considerations together, we conclude that the size of the ΔF_{max} signal at A52C correlates directly with the magnitude of an agonist-induced conformational change that enables flipping to take place. Glycine produces the largest conformational change; hence it produces the fastest isomerization rate to the flipped state. Because glycine produces the largest affinity increase in the flip state, we propose that the magnitude of this conformational change is directly related to the agonist affinity to the flip state. The conservative A52S mutation inhibits this conformational change from occurring via a specific local interaction. This supports our conclusion that the agonist-specific pre-flip conformation change is occurring in the immediate environment of Ala-52.

ΔF Responses Exhibit Reduced Cooperativity—A general feature of all mutants investigated here is that ΔF dose responses exhibit substantially lower cooperativity than ΔI dose responses. Indeed, for most cases the n_H value for ΔF dose responses was not significantly different to 1 (Table 1). Our interpretation is that the fluorophores are reporting conformational changes induced by individual agonist binding events in activated receptors. This implies that the closed-flip transition occurs within individual subunits and is not cooperative. Such an interpretation is consistent with Plested *et al.* (33) who concluded that the closed-flip conformational change may be responsible for propagating agonist-mediated conformational changes between subunits and that the A52S mutation may disrupt these interactions. Mukhtasimova *et al.* (37) proposed that flipping in the nAChR also occurs independently in each subunit.

Local Conformational Changes in Domains Flanking the Outer β-Sheet—Finally, it is relevant to consider differences in responses of labeled residues in the inner β-sheet with those attached to domains flanking the outer β-sheet (*i.e.* loops C and

F and pre-M1). As ΔF_{max} signals in loops C and F and the pre-M1 domain were agonist-independent, we propose that agonist efficacy information is transduced via the inner β-sheet only.

A recent study on the nAChR found that the flip state was induced by the closure of loop C (37). However, our results suggest that agonist efficacy is not encoded by movements of this domain. To reconcile both sets of results, we propose that loop C closure not only induces flip but alters the interaction between the bound agonist and loops D and E. Movements leading to large ΔF responses in loops D and E that are induced by low efficacy agonists may actually serve to prevent or limit the movement of loop 2. Because movements in loop F and the pre-M1 domain are not agonist-dependent, we propose they may occur in parallel with the C loop perhaps via the outer β-sheet moving as a rigid body.

Another aspect of domain-specific movements is that while the inner β-sheet clearly discriminates between different agonists, labeled residues in loops D and E show little or no discrimination between taurine and strychnine. How, then, does the receptor discriminate these two compounds with very distinct effects on the channel? The answer seems to lie in regions flanking the outer β-sheet: loop C and the pre-M1 domain show no discrimination between different agonists, but some parts of loop C and a number of residues in the pre-M1 domain clearly respond differently to antagonists (27). However, more experiments are needed to further elucidate this intricate interplay between the inner and outer β-sheets of the GlyR LBD.

In conclusion, our results suggest that a closed-flip state conformation change, with a magnitude proportional to the agonist affinity increase in the flip state, occurs in the immediate microenvironment of Ala-52. We suggest this conformational change may not be cooperative but may lead to intersubunit cooperativity. Understanding the structural basis of this conformational change may help explain why the GlyR responds differently to high and low efficacy agonists. This information could eventually prove useful for designing novel Cys-loop receptor-targeted partial agonist drugs for a variety of neurological disorders (38).

REFERENCES

1. Lynch, J. W. (2004) *Physiol. Rev.* **84,** 1051–1095
2. Bocquet, N., Nury, H., Baaden, M., Le Poupon, C., Changeux, J. P., Delarue, M., and Corringer, P. J. (2008) *Nature* **457,** 111–114
3. Brejc, K., van Dijk, W. J., Klaassen, R. V., Schuurmans, M., van Der Oost, J., Smit, A. B., and Sixma, T. K. (2001) *Nature* **411,** 269–276
4. Hilf, R. J., and Dutzler, R. (2008) *Nature* **452,** 375–379
5. Hilf, R. J., and Dutzler, R. (2008) *Nature* **457,** 115–118
6. Miyazawa, A., Fujiyoshi, Y., and Unwin, N. (2003) *Nature* **423,** 949–955
7. Lewis, T. M., Schofield, P. R., and McClellan, A. M. (2003) *J. Physiol.* **549,** 361–374
8. Schmieden, V., Kuhse, J., and Betz, H. (1992) *EMBO J.* **11,** 2025–2032
9. De Saint Jan, D., David-Watine, B., Korn, H., and Bregestovski, P. (2001) *J. Physiol.* **535,** 741–755
10. Schmieden, V., and Betz, H. (1995) *Mol. Pharmacol.* **48,** 919–927
11. Grudzinska, J., Schemm, R., Haeger, S., Nicke, A., Schmalzing, G., Betz, H., and Laube, B. (2005) *Neuron* **45,** 727–739
12. Burzomato, V., Beato, M., Groot-Kormelink, P. J., Colquhoun, D., and Sivilotti, L. G. (2004) *J. Neurosci.* **24,** 10924–10940
13. Lape, R., Colquhoun, D., and Sivilotti, L. G. (2008) *Nature* **454,** 722–727
14. Pless, S. A., and Lynch, J. W. (2008) *Clin. Exp. Pharmacol. Physiol.* **35,** 1137–1142
15. Mannuzzu, L. M., Moronne, M. M., and Isacoff, E. Y. (1996) *Science* **271,** 213–216
16. Chang, Y., and Weiss, D. S. (2002) *Nature Neurosci.* **5,** 1163–1168
17. Dahan, D. S., Dibas, M. I., Petersson, E. J., Auyeung, V. C., Chanda, B., Bezanilla, F., Dougherty, D. A., and Lester, H. A. (2004) *Proc. Natl. Acad. Sci. U.S.A.* **101,** 10195–10200
18. Mourot, A., Bamberg, E., and Rettinger, J. (2008) *J. Neurochem.* **105,** 413–424
19. Muroi, Y., Czajkowski, C., and Jackson, M. B. (2006) *Biochemistry* **45,** 7013–7022
20. Pless, S. A., Dibas, M. I., Lester, H. A., and Lynch, J. W. (2007) *J. Biol. Chem.* **282,** 36057–36067
21. Khatri, A., Sedelnikova, A., and Weiss, D. S. (2009) *Biophys. J.* **96,** 45–55
22. Muroi, Y., Theusch, C. M., Czajkowski, C., and Jackson, M. B. (2009) *Biophys. J.* **96,** 499–509
23. Pless, S. A., and Lynch, J. W. (2009) *J. Neurochem.* **108,** 1585–1594
24. Rajendra, S., Lynch, J. W., Pierce, K. D., French, C. R., Barry, P. H., and Schofield, P. R. (1995) *Neuron* **14,** 169–175
25. Taleb, O., and Betz, H. (1994) *EMBO J.* **13,** 1318–1324
26. Pless, S. A., Millen, K. S., Hanek, A. P., Lynch, J. W., Lester, H. A., Lummis, S. C., and Dougherty, D. A. (2008) *J. Neurosci.* **28,** 10937–10942
27. Pless, S. A., and Lynch, J. W. (2009) *J. Biol. Chem.* **284,** 15847–15856
28. Beato, M., Groot-Kormelink, P. J., Colquhoun, D., and Sivilotti, L. G. (2002) *J. Gen. Physiol.* **119,** 443–466
29. Beato, M., Groot-Kormelink, P. J., Colquhoun, D., and Sivilotti, L. G. (2004) *J. Neurosci.* **24,** 895–906
30. Chang, Y., and Weiss, D. S. (1999) *Nature Neurosci.* **2,** 219–225
31. Hansen, S. B., Sulzenbacher, G., Huxford, T., Marchot, P., Taylor, P., and Bourne, Y. (2005) *EMBO J.* **24,** 3635–3646
32. Wagner, D. A., and Czajkowski, C. (2001) *J. Neurosci.* **21,** 67–74
33. Plested, A. J., Groot-Kormelink, P. J., Colquhoun, D., and Sivilotti, L. G. (2007) *J. Physiol.* **581,** 51–73
34. McLaughlin, J. T., Fu, J., and Rosenberg, R. L. (2007) *Mol. Pharmacol.* **71,** 1312–1318
35. Jin, R., Banke, T. G., Mayer, M. L., Traynelis, S. F., and Gouaux, E. (2003) *Nature Neurosci.* **6,** 803–810
36. Celie, P. H., van Rossum-Fikkert, S. E., van Dijk, W. J., Brejc, K., Smit, A. B., and Sixma, T. K. (2004) *Neuron* **41,** 907–914
37. Mukhtasimova, N., Lee, W. Y., Wang, H. L., and Sine, S. M. (2009) *Nature* **459,** 451–454
38. Hogg, R. C., and Bertrand, D. (2007) *Biochem. Pharmacol.* **73,** 459–468